npj | science of food

Article

Published in partnership with Beijing Technology and Business University & International Union of Food Science and Technology

https://doi.org/10.1038/s41538-025-00503-x

Phytochemical profiling, antioxidant properties, and anticancer activity of *Pourouma cecropiifolia* Mart. from the Ecuadorian Amazon

Carlos Méndez-Durazno[1], Pablo A. Cisneros-Pérez[2,3], Noroska G. S. Mogollón[3], Jose R. Mora[4], Sebastián A. Cuesta[4,5], Natalia Bailón-Moscoso[6], Juan Carlos Romero-Benavides[7], Raúl Monge-Sevilla[1], Lenys Fernández[1], David Romero-Estévez[8] & Patricio J. Espinoza-Montero[1] ✉

Some fruits are used as promising anticancer agents due to their antioxidant and antimutagenic properties. This work explores the potential of the fruit of *Pourouma cecropiifolia* Mart. as a source of compounds with anticancer activity. The research covers: (i) phytochemical profiling of hydroethanolic extracts from the peel, pulp, and seeds of *P. cecropiifolia* Mart. using liquid ultra-performance chromatography quadrupole time-of-flight mass spectrometry (UPLC-QTOF-MS); (ii) evaluation of antioxidant and anticancer potential of the extracts against carcinoma cell lines (HeLa, RKO, MCF-7, and T47D); and (iii) in silico docking analyses with human cytochrome P450 1A1 (CYP 1A1) and CYP 1B1. A total of 18 compounds were tentatively identified by UPLC-QTOF-MS, including flavonoids, phenolic glycosides, lignans, phenolic acids, terpenes, iridoid glycosides, proanthocyanidins, curcuminoids, and naphthodianthrone. Molecular docking simulations identified nortracheloside and epicatechin as potential inhibitors of CYP 1A1 and CYP 1B1, suggesting cytotoxic activity. The antiproliferation assay showed that pulp extracts had moderate activity against human breast ductal cancer cells.

Cancer is among the leading causes of death worldwide, with 19.3 million new cases and 10.0 million deaths reported in 2020[1]. Breast cancer in particular is rising in prevalence, with an estimated 2.3 million new global cases, according to the Global Cancer Statistics 2020 report[2,3]. Despite advancements in cancer diagnosis and treatment, barriers to clinical care and predictive diagnosis persist. Multimodal treatment approaches, including radiation, surgery, and chemotherapy, remain the standard for managing advanced cancer[4]. However, these treatments are often inadequate, as they cannot eliminate all cancer cells, necessitating the development of alternative therapies.

Research has shown natural products to be promising alternative anticancer treatments[2,5,6]. Many plant-derived bioactive molecules have the potential to contribute to the medical, agricultural, and nutritional fields[7]. Phytochemicals, which are specialized metabolites, are known to modulate multiple biological pathways in living tissue, offering a range of benefits, such as antioxidant, antimicrobial, anti-inflammatory, anti-diabetic, and anti-cancer properties[8]. These phytochemicals are categorized into major classes—phenolic compounds, carotenoids, alkaloids, terpenes, vitamins, and anthocyanins—based on their physiochemical properties, distribution in nature, and biosynthetic pathways[9].

The Amazon rainforest, one of the world's most biodiverse areas, is home to approximately 40,000 plant species[10]. In particular, Ecuador is recognized as one of 17 megadiverse countries owing to its high plant and animal biodiversity[11]. Many of its botanical species remain underexplored

[1]Escuela de Ciencias Químicas, Pontificia Universidad Católica del Ecuador, Quito, Ecuador. [2]Grupo de Investigación Aplicada en Materiales y Procesos (GIAMP), School of Chemical Sciences and Engineering, Yachay Tech University, Urcuqui, Ecuador. [3]Biomolecules Discovery Group, Universidad Regional Amazónica Ikiam, Tena, Ecuador. [4]Departamento de Ingeniería Química, Universidad San Francisco de Quito, Diego de Robles y Vía Interoceánica, Quito, Ecuador. [5]Department of Chemistry, Manchester Institute of Biotechnology, The University of Manchester, Manchester, UK. [6]Departamento de Ciencias de la Salud, Universidad Técnica Particular de Loja, San Cayetano Alto, Loja, Ecuador. [7]Departamento de Química, Facultad de Ciencias Exactas y Naturales, Universidad Técnica Particular de Loja, Loja, Ecuador. [8]Centro de Estudios Aplicados en Química (CESAQ), Pontificia Universidad Católica del Ecuador, Quito, Ecuador. ✉e-mail: pespinoza646@puce.edu.ec

for their phytochemical composition. Among these, the Cecropiaceae family has shown considerable potential given its phenolic compound-rich chemical profile[12–14].

In this context, *Pourouma cecropiifolia* Martius (commonly known as *uvilla*, *uva de monte*, and *orsacha uvillas*)[15] was selected for investigation. This tropical plant, native to the Ecuadorian Amazon (distributed throughout the Pastaza, Sucumbíos, Napo, Zamora Chinchipe, and Morona Santiago provinces) at altitudes of 200–900 masl, produces sweet, juicy fruit typically consumed fresh or made into jams and wine[16]. The immature fruits are green, which turn purple after ripening. Fruits are spherical drupes 2–4 cm in diameter with a sweet, mucilaginous flesh containing one seed[14]. However, its susceptibility to mechanical damage and high perishability pose challenges for broader commercial use[17].

Previous studies have partially characterized the phenolic profile of *P. cecropiifolia* Mart. (Cecropiaceae), identifying compounds such as rutin, quercetin derivatives, catechin, epicatechin, procyanidin B, and four hydroxycinnamic acid derivatives[16]. Notably, peel extracts of *P. cecropiifolia* Mart. have shown cytotoxic effects on cancer cell lines[16]. However, comprehensive data on the chemical composition and biological activities of hydroethanolic extracts from the peel and seed remain limited. This study aims to address these gaps by investigating the cytotoxic and antioxidant activity of hydroethanolic extracts made from *P. cecropiifolia* Mart. pulp, peel, and seeds and profiling their bioactive compounds using ultra-performance liquid chromatography quadrupole time-of-flight mass spectrometry (UPLC-QTOF-MS). The findings contribute to a deeper understanding of the potential applications of *P. cecropiifolia* Mart. in nutraceutical development.

Results and discussion

Bioactive compounds

Flavonoids and phenolic compounds derived from botanical sources are well-known for their extensive pharmacological activities[18,19]. As shown in Table 1, TPC ranged from 0.30 ± 0.01 to 23.18 ± 0.04 mg gallic acid equivalent (GAE) g^{-1}, flavonoids 1.02 to 2.3 mg quercetin equivalent (QE) g^{-1}, yellow flavonoids from 0.69 to 1.46 mg QE g^{-1}, and anthocyanin from 0.16 ± 0.00 to 8.43 ± 0.04 mg g^{-1} d.w. Among the fruit parts, seeds exhibited the highest total TPC (23.18 ± 0.04 mg GAE g^{-1}) and flavonoid content (0.31 ± 0.00 mg QE g^{-1} d.w.). The highest anthocyanin content (8.43 ± 0.040 mg g^{-1}) was observed in the peel extract, while pulp exhibited the lowest TPC (0.30 ± 0.01 mg GAE g^{-1}) and total flavonoid content (0.03 ± 0.00 mg QE g^{-1}). The overall phenolic content of the fruit was higher than the flavonoid content. In contrast to our findings, Luts et al.[16] found anthocyanins primarily in the peel of *P. cecropiifolia* Mart., and Ordonez et al.[20] reported high TPC in its peel and seeds. We observed slightly higher TPC and total anthocyanin content in the seed extract, which is possibly attributable to variations in cultivars, climatic conditions, fruit ripeness stage, and the type of extraction solvent used.

The chromatographic analysis of extracts from the peel, pulp, and seed of *P. cecropiifolia* Mart. revealed the presence of ascorbic acid and *trans*-resveratrol. Ascorbic acid is an essential nutrient that serves as a cofactor for collagen prolyl hydroxylases, playing a crucial biological role[21]. It exhibits notable antioxidant[22] and anticancer[23–25] properties, including enhancing TET2 dioxygenase activity in myeloid neoplasia[26]. According to the results, ascorbic acid was detected exclusively in the *P. cecropiifolia* Mart. peel extract (4.67 ± 0.28 mg 100 g^{-1} d.w.) (Table 1). The ascorbic acid content was comparable to levels found in fruits such as *Pyrus communis* L. (2.8 mg 100 g^{-1}), *Eriobotrya japonica* Lindl. (3.2 mg 100 g^{-1}), and *Eugenia malaccensis* L. (3.8 mg 100 g^{-1})[27].

Trans-Resveratrol (3,4′,5-trihydroxystilbene), a stilbenoid polyphenol, is widely distributed among plant taxa, including grape, pine, blueberry, cranberry, bilberry, and peanuts[28]. It exhibits diverse pleiotropic health benefits against various chronic diseases[29–31], and in-vitro screening has identified it as a first-generation sirtuin-activating compound[32] that activates nicotinamide adenine dinucleotide-dependent silent information regulator 2 (SIR2) deacetylase[33], contributing to its therapeutic effects.

For the first time, this study identified the presence of *trans*-resveratrol in *P. cecropiifolia* Mart. using UPLC-ESI-QTOF-MS analysis. Deprotonated [M–H] ions were identified at m/z 227.97 (Fig. 1). The highest *trans*-resveratrol concentration was found in the peel extract (21.00 ± 0.30 μg g^{-1}), with lower levels detected in the pulp (2.60 ± 0.00 μg g^{-1}) and none in the seeds. Comparatively, the *trans*-resveratrol content in the peel of *P. cecropiifolia* Mart. was higher than that found in the peels of *Vitis labrusca* (3.54 μg g^{-1}) and *Syzygium cumini* L. (11.19 μg g^{-1})[34]. However, higher *trans*-resveratrol levels have been reported in *M. rubra* fruit (50.61 μg g^{-1} d.w.)[34]. Together, these findings suggest that the *trans*-resveratrol and ascorbic acid identified in *P. cecropiifolia* Mart. are promising bioactive compounds that contribute to its antioxidant capacity.

Untargeted metabolic profiling

Peel, pulp and seeds extracts from *P. cecropiifolia* Mart. were analyzed using UPLC-QTOF-MS. The total ion chromatograms obtained in negative ionization modes are presented in Fig. 2, while Table 2 summarizes the tentative identification of metabolites, including molecular ions $[M–H]^-$, retention times (min), accurate masses, and ion molecular formulas. The analysis revealed the tentative identification of 18 metabolites as predominant compounds in the peel, pulp, and seed extracts, including flavonoids (7), phenolic glycosides (1), lignans (2), phenolic acids (1), terpenes (1), iridoid glycosides (1), proanthocyanidins (2), curcuminoids (1), and naphthodianthrone (1).

Flavonoids

Three flavonoids (1, 2, and 4) were tentatively identified in the peel extract. Compound 1, with a retention time (t_R) of 3.03 min, exhibited a deprotonated molecular ion $[M-H]^-$ at m/z 909.2027 and was identified as carthamin. Compound 2 displayed $[M-H]^-$ at m/z 547.1420, with typical fragment ions at m/z 437.08740, 143.03290, and 329.08650; this compound was tentatively identified as mirificin ($C_{26}H_{28}O_{13}$). Compound 4, with $[M-H]^-$ at m/z 289.0714 (R_t = 7.18 min), was characterized as (-)-epicatechin.

Four additional flavonoids were tentatively identified in the seed extracts of *P. cecropiifolia* Mart. Compound 12 exhibited $[M-H]^-$ at 433.0768, with fragmentations at m/z 303.08185, 343.07626, and 373.10287, and was identified as quercetin-3-arabinopyranoside. Fraisse et al.[35] isolated quercetin-3-arabinopyranoside from *Alchemilla xanthochlora*, a well-known medicinal plant recognized for its anti-inflammatory and astringent properties[36]. Furthermore, this compound has been reported as an α-glucosidase inhibitor[37]. Compound 13, with an t_R of 7.04 min, displayed a

Table 1 | Total flavonoid, anthocyanin, ascorbic acid, and *trans*-resveratrol content of hydroethanolic extracts of *P. cecropiifolia* Mart. (peel, pulp, and seed)

	Total flavonoids content (QE mg g^{-1}d.w.)	Total anthocyanin content (mg g^{-1} d. w.)	Ascorbic acid (mg 100 g^{-1} d.w.)	*Trans*-resveratrol (μg g^{-1}d.w.)
Peel	0.13 ± 0.00^b	8.43 ± 0.04^a	4.67 ± 0.28^a	21.00 ± 0.30^a
Pulp	0.03 ± 0.00^c	0.16 ± 0.00^c	0.00 ± 0.00^b	2.60 ± 0.00^b
Seed	0.31 ± 0.00^a	1.8 ± 0.00^b	0.00 ± 0.00^b	0.00 ± 0.00^c

Values are expressed as mean ± SD (n = 3). Superscript lowercase letters ("a", "b", "c") within the same column indicate statistically significant differences among the different parts of *P. cecropiifolia* (peel, pulp, and seed), as determined by Tukey's multiple comparisons test ($p > 0.05$).

deprotonated molecule at m/z 503.1227 and was tentatively identified as neocomplanoside based on electrospray ionization (ESI)-MS^2 analysis. The negative ESI-MS spectrum of Compound 16 generated a molecular ion peak $[M–H]^-$ at 579.1704 (R_t = 11.24 min) and was identified as naritutin, a compound previously reported in citrus species[38]. Finally, in the MS spectrum, Compound 17 was noted with $[M–H]^-$ at m/z 610.1932 ($C_{28}H_{34}O_{15}$) and was identified as neohesperidin.

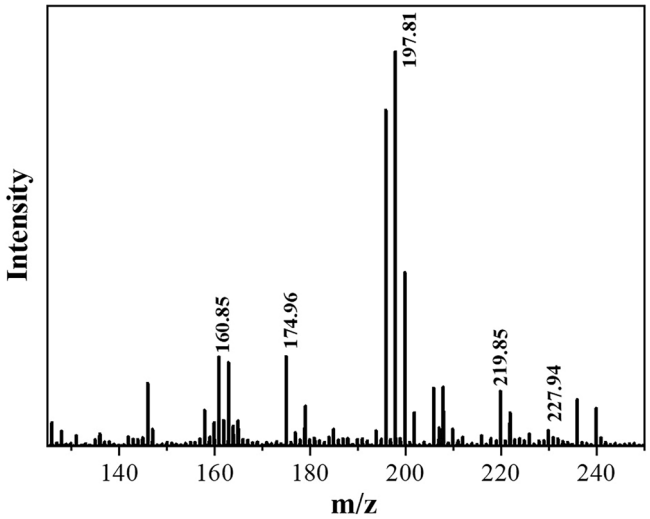

Fig. 1 | Mass spectrometry spectrum of *trans*-resveratrol from the peel extract from *P. cecropiifolia* Mart.

Lignans

Two lignans were tentatively identified in this study. The negative ESI-MS spectrum of the reference standard neoolivil-4-O-glucopyranoside (Compound 3), a deprotonated molecular ion, was detected at m/z 353.0875 (t_R = 5.88 min) ($C_{26}H_{33}O_{11}$). Similarly, the UPLC-ESI-QTOF-MS analysis identified nortracheloside (Compound 5) with a deprotonated ion at m/z 535.1826 (t_R = 10.66 min) ($C_{26}H_{32}O_{12}$). A peak in the negative ESI mode at t_R = 10.66 min with $[M–H]^-$ at m/z 355.1627 was identified as denudatin B (Compound 5), previously reported as a nitric oxide synthase inhibitor[39]. According to the literature, nortracheloside exhibits anticancer properties[40].

Proanthocyanidins

Two proanthocyanidins were tentatively identified in the *P. cecropiifolia* Mart. extracts. The negative ESI-MS spectrum of procyanidin B2 (Compound 9) at t_R = 6.73 min showed a deprotonated molecular ion at m/z 577.1350. Procyanidin B2 has been reported to exhibit antioxidative, anti-inflammatory, and antitumor activity[41]. Mahuannin J (Compound 10), detected with $[M–H]^-$ at m/z 555.0951, showed parent ions at m/z 334.01500 and 391.04033.

Phenolic acid

According to the MS spectra, $[M–H]^-$ at m/z 353.0876 and two parent ions at m/z 191.05595 and 179.03457 correspond to chlorogenic acid (CGA). This compound, also found in tea and green coffee extracts, is synthesized by plants via the shikimic acid pathway. CGA was first isolated from coffee beans by K. Freudenberg in 1920[42], with its structure identified as 3-O-

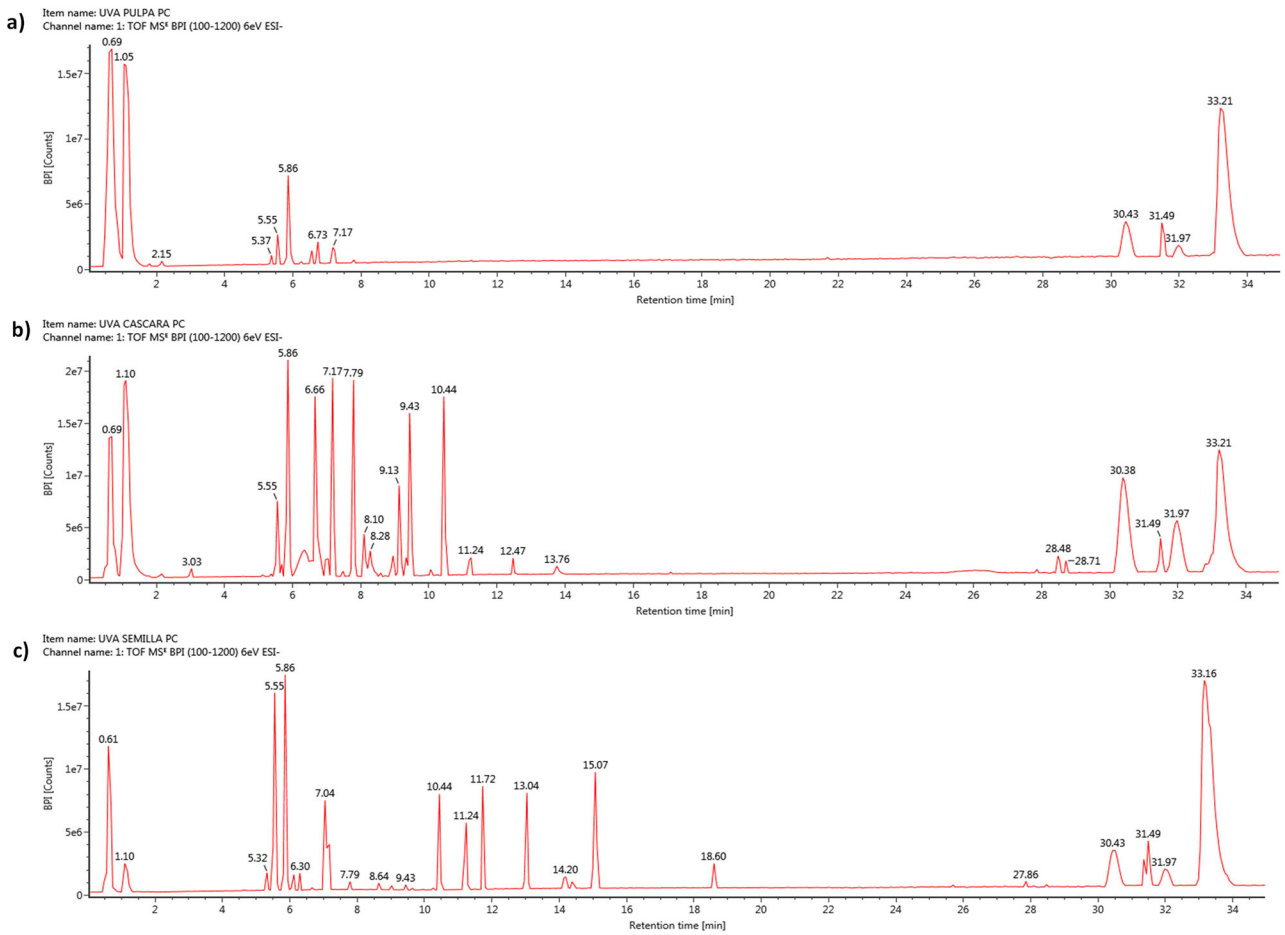

Fig. 2 | Total ion chromatogram of *P. cecropiifolia* Mart. a Peel, **b** pulp, and **c** seed extracts in negative ion mode.

Table 2 | Characterization of metabolites in *P. cecropiifolia* Mart. extracts using UPLC-ESI-QTOF-MS

Part of fruit	Sr. #	error ppm	Chemical Formula	Observed m/z	R_t (min)	Ions fragments	Adducts	Preliminary identified compounds	Biological activity
Peel	1	−7.5	$C_{43}H_{42}O_{22}$	909.2027	3.03	455.06115 201.83439	-H	Carthamin	Antioxidant and Neuroprotective Activities[35]
	2	−6.8	$C_{26}H_{28}O_{13}$	547.1420	5.55	437.08740 143.03290 329.08650	-H	Mirificin	Tyrosinase inhibitors[36]
	3	−0.9	$C_{26}H_{33}O_{11}$	353.0875	5.88	191.05575 189.01857	-H	Neoolivil-4-O-glucopyranoside	-
	4	−1.1	$C_{15}H_{14}O_6$	289.0714	7.18	289.07134 161.02870 577.13503	-H	(-)-Epicatechin	Antioxidant[37]
	5	0.9	$C_{26}H_{32}O_{12}$	535.1826	10.66	179.03438 161.02364 466.13509	-H	(-)-Nortracheloside	Anticancer[38]
	6	−9.7	$C_{15}H_{20}O_4$	263.1263	11.31	179.10685 198.03467	-H	(-)-Istanbulin A	Antitumoral[39]
	7	1	$C_{21}H_{24}O_5$	355.1627	24.32	353.27168 297.15229	-H	(-)- Denudatin B	Inhibitory activity on nitric oxide (NO) production[40]
Pulp	8	1.1	$C_{15}H_{18}O_9$	341.1024	5.35	221.04499 179.03449 281.06583	-H	Caffeic acid 3-hexoside	Treatment of obesity (hydroxycinnamic acid and derivatives)[41]
	1	1.7	$C_{43}H_{42}O_{22}$	909.2110	5.86	179.03457 351.07141 353.08745 375.06825	-H	Carthamin	Antioxidant and Neuroprotective[35]
	9	−0.3	$C_{30}H_{26}O_{12}$	577.1350	6.73	298.07134 407.07689 425.08697	-H	Procyanidin B2	Antioxidant, anti-inflammatory and antitumoral[42]
Seed	5	−6.7	$C_{26}H_{32}O_{12}$	535.1789	5.55	289.07123 303.12082	-H	Nortracheloside	Anticancer[43]
	10	3.3	$C_{30}H_{24}O_9$	555.0951	5.86	334.01500 391.04033	-H	Mahuannin J	-
	11	−0.5	$C_{16}H_{18}O_9$	353.0876	5.89	191.05595 179.03457	-H	Chlorogenic acid	Antioxidant and DNA protective compounds[44]
	12	−2.0	$C_{20}H_{18}O_{11}$	433.0768	6.10	303.08185 343.07626 373.10287	-H	Quercetin-3-arabinopyranoside	α glucosidase inhibitor[45]
	13	6.4	$C_{24}H_{24}O_{12}$	503.1227	7.04	337.09174 474.07450	-H	Neocomplanoside	-
	14	−7.5	$C_{18}H_{22}O_{11}$	413.1058	7.79	191.05557 245.04474	-H	Asperuloside	Antioxidant[46]
	15	1.1	$C_{30}H_{30}O_{14}$	613.1599	8.64	295.02629 269.04433	-H	Safflomin C	Antithrombotic[47]
	16	−1.9	$C_{27}H_{32}O_{14}$	579.1704	11.24	173.04516 353.08717	-H	Narirutin	Anti-inflammatory[48]
	17	1.1	$C_{28}H_{34}O_{15}$	610.1932	15.10	285.03963 456.07185 507.18652	-H	Neohesperidin	Hypoglycemic and hypolipidemic effects[49]
	18	−3.3	$C_{30}H_{18}O_8$	505.0912	27.86	358.04000	-H	Protohypericin	Anti-influenza[50]

UPLC-ESI-QTOF-MS ultra-performance liquid chromatography with electrospray ionization quadrupole time-of-flight mass spectrometry.

caffeoylquinic acid by Fischer and Dangschat in 1932[43]. In clinical settings, chlorogenic acid exhibits multiple pharmacological properties, including antimicrobial, hepatoprotective, anticancer, immunomodulatory, DNA protective, neuroprotective, antioxidant, and antidiabetic activities[44–46]. Many in vitro and in vivo studies have also demonstrated that CGA has a pharmacological effect against myocardial ischemia–reperfusion injury[47].

Antioxidant capacity

Antioxidants are compounds that scavenge highly reactive oxygen species, preventing chain reactions that can damage cell components such as proteins, DNA, and membrane phospholipids[48]. The literature has extensively documented the substantial contribution of various phytochemical components to the antioxidant activity (AA) of fruits, with phenolic compounds recognized as key contributors[49–51]. In this study, the antioxidant capacity of *P. cecropiifolia* Mart. was evaluated using different assays—the 2,2-diphenyl-1-picrylhidrazyl (DPPH), 2,2'-azino-bis(3-ethylbenzothiazoline-6-sulfonic acid) (ABTS), and ferric reducing antioxidant power (FRAP) assays—as well as electrochemical methods measuring the antioxidant index 50 value (AI_{50}) and electrochemical index (EI) to provide a comprehensive assessment of its antioxidant potential.

Table 3 shows the free radical scavenging activity of the hydroethanolic extracts from the peel, pulp, and seed of *P. cecropiifolia* Mart. Among the extracts, the seed and peel displayed the highest AA. Potential AA was quantified using the Trolox equivalent antioxidant capacity (TEAC) assay

Table 3 | Antioxidant properties of hydroethanolic extracts of *P. cecropiifolia* Mart

Part of fruit	EI (μA V^{-1})	AI_{50} (mg L^{-1})	TPC (mg GAE g^{-1} d.w.)	FRAP (mmol Fe^{2+} g^{-1} d.w.)	$TEAC_{DPPH}$	$TEAC_{ABTS}$
Peel	11.63 ± 0.1[a]	1.53 ± 0.03[b]	0.67 ± 0.01[b]	0.011 ± 0.00[b]	4.57 ± 0.03[b]	7.10 ± 0.10[b]
Pulp	3.81 ± 0.00[c]	1.60 ± 0.03[a]	0.30 ± 0.01[c]	0.014 ± 0.00[b]	1.34 ± 0.01[b]	2.70 ± 0.01[c]
Seed	14.19 ± 0.1[b]	0.75 ± 0.02[c]	23.18 ± 0.04 [a]	0.402 ± 0.01[a]	212.61 ± 2.92[a]	350.60 ± 2.20[a]

ABTS 2,2'-azino-bis(3-ethylbenzothiazoline-6-sulfonic acid), AI_{50} antioxidant index 50, *DPPH* 2,2-diphenyl-1-picrylhidrazyl, *d.w.* dry weight, *EI* electrochemical index, *FRAP* ferric reducing antioxidant power, *GAE* gallic acid equivalent, *TEAC* Trolox equivalent antioxidant capacity, *TPC* total polyphenol content.
Values are expressed as mean ± SD ($n = 3$). Superscript lowercase letters ("a", "b", "c") within the same column indicate statistically significant differences among the different parts of *P. cecropiifolia* (peel, pulp, and seed), as determined by Tukey's multiple comparisons test ($p < 0.05$).

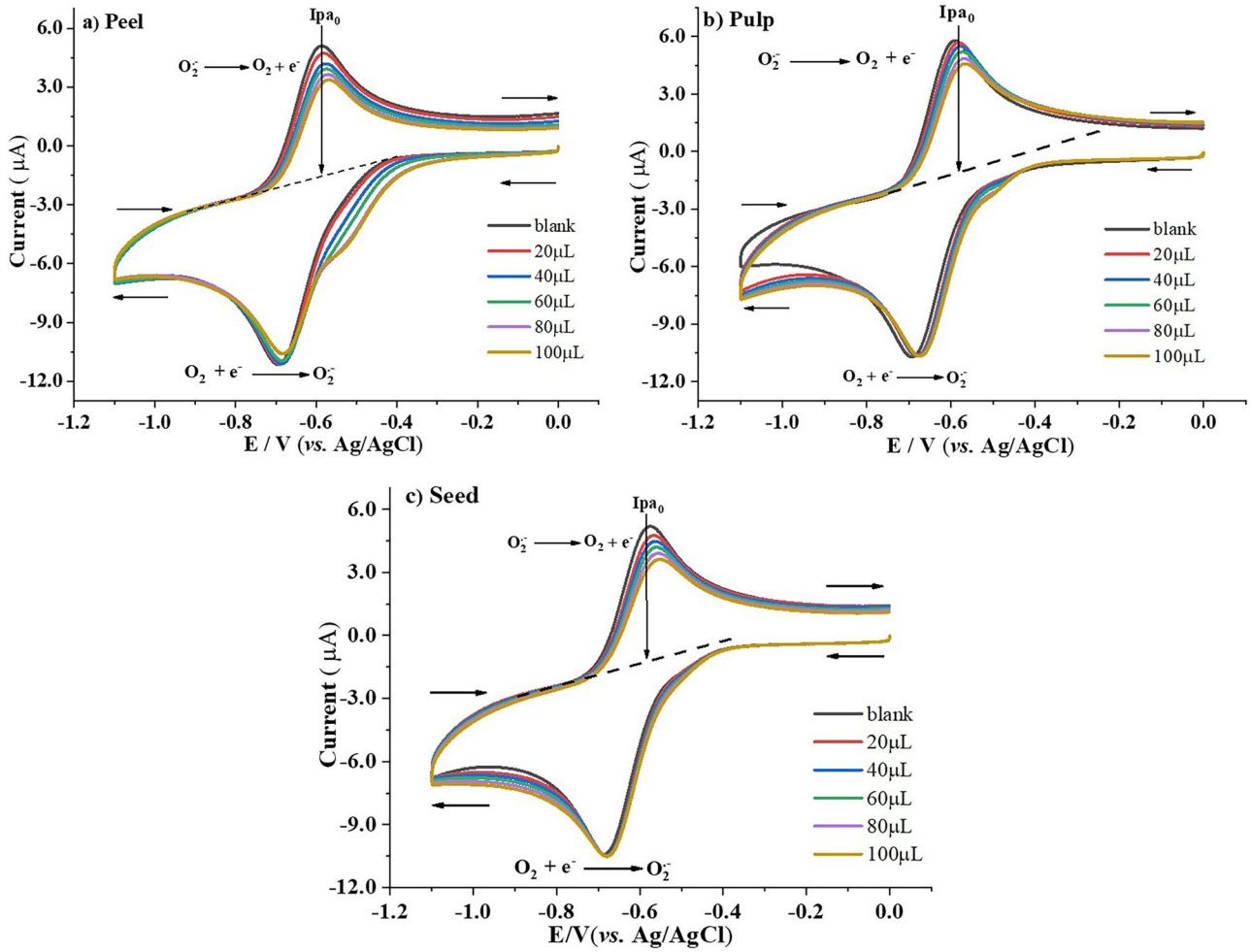

Fig. 3 | Cyclic voltammograms of the $O_2/O_2^{\bullet-}$ system in the presence of increasing concentrations of *P. cecropiifolia* Mart. Measurements were performed in DMS + Bu_4NPF_6 0.05 M at a scan rate of 0.1 V s^{-1}, glassy carbon as work electrode. **a** Peel, **b** pulp, and **c** seed.

value. These values determined by the DPPH assay ranged from 1.34 ± 0.01 to 212.61 ± 2.92, while those obtained with the ABTS assay ranged from 2.70 ± 0.01 to 350.60 ± 2.20. The extracts' antioxidant capacities obeyed the following order: seed > peel > pulp. The AA of *P. cecropiifolia* Mart. was further evaluated using the FRAP assay, which measures the ability of the extracts to reduce Fe(III) to Fe(II). The FRAP values ranged from 0.011 to 0.402 ± 0.010 mmol Fe^{2+} g^{-1} d.w. As shown in Table 3, the pulp extract demonstrated the lowest AA, whereas the seed extract showed the highest. Notably, the seed and peel extracts from *P. cecropiifolia* Mart. exhibited significant AA, in contrast to the results of previous studies[20].

Phytochemicals are electroactive compounds with small redox potentials, reflecting their AA. Electrochemical methods are practical, rapid, and complementary tools for evaluating AA given their high sensitivity and low detection limits[52]. Figure 3 presents the cyclic voltammograms of $O_2^{\bullet-}$ in the absence (blank) and presence of hydroethanolic extracts of *P. cecropiifolia* Mart.

In Fig. 3a, b, c the anodic peak current intensity of the voltammograms decreases significantly upon the addition of *P. cecropiifolia* Mart. ethanolic extracts (peel, pulp, and seed). This decrease is because the $O_2^{\bullet-}$ formed by the reduction of O_2 reacts with molecules in the extracts possessing antioxidant properties, resulting in a reduced oxidation signal of $O_2^{\bullet-}$ to O_2[53]. From the voltammograms in Fig. 3, the AI_{50} values were calculated by fitting the plot of $((Ip_a^0 - Ip_a^s)/Ip_a^0)$ versus the extract concentration (Fig. 4). According to Table 3, the seed extract exhibited the lowest AI_{50} value (0.75 ± 0.02 mg L^{-1}), followed by the peel (1.53 ± 0.03 mg L^{-1}) and pulp (1.60 ± 0.03 mg L^{-1}). Overall, the cyclic voltammetry (CV) analysis demonstrates the seed extract of *P. cecropiifolia* Mart. is a promising source of antioxidants with strong superoxide radical scavenging activity. It is

noteworthy that lower AI_{50} values corresponded to higher antioxidant properties of the sample.

To further investigate the antioxidant properties of hydroethanolic extracts of *P. cecropiifolia* Mart., the EI was determined using differential pulse voltammetry (DPV). Figure 5. reveals an anodic peak with a slight shoulder for the seed extract between 0.235 and 0.546 V (*vs.* Ag/AgCl), while the peel extract signal extends from 0.323 to 0.638 V (*vs.* Ag/AgCl), and that for the pulp from 0.409 to 0.766 V (*vs.* Ag/AgCl). Lower potential (E_{pa} < 0.45 V) values correspond to species with high capacity for electron donation, indicating higher AA[54]. Thus, the electroactive molecules in the *P. cecropiifolia* Mart. seed extract exhibits greater AA, as they react at lower potentials. The EI results are summarized in Table 3; EI values ranged from 3.81 ± 0.00 to 14.19 ± 0.10 μA V^{-1}. The seed extract demonstrated the highest antioxidant potential, which is consistent with the results of the FRAP, $TEAC_{DPPH}$, and $TEAC_{ABTS}$ analyses.

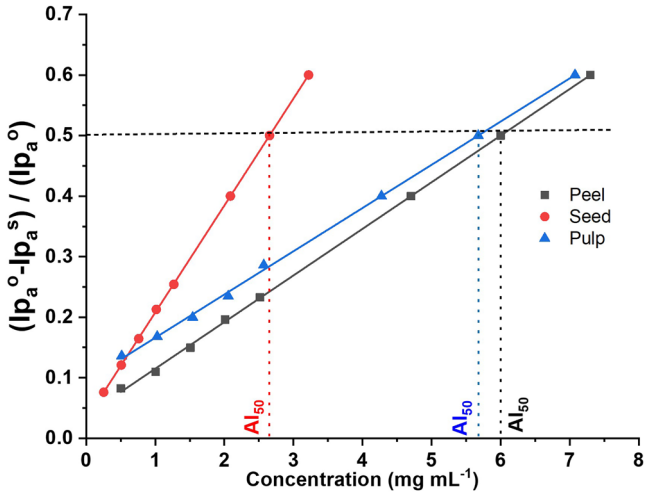

Fig. 4 | Dimensionless parameter $((Ip_a^0 - Ip_a^s)/Ip_a^0)$ related to the decrease in $O_2^{\bullet-}$ current vs. the concentration of *P. cecropiifolia* Mart. extracts.

Correlation analysis

Phenolic compounds have been shown to exhibit a positive relationship with AA[55,56]. Pearson's correlation coefficients between total polyphenol content (TPC) and AA assays are presented in Table 4. The analysis revealed a strong positive linear relationship between TPC and AA assays of *P. cecropiifolia* Mart. (TPC-$TEAC_{DPPH}$: $R^2 = 1.000$; TPC-$TEAC_{ABTS}$:

Table 4 | Pearson's correlation coefficients between TPC and antioxidant capacity assays

	TPC	$TEAC_{DPPH}$	$TEAC_{ABTS}$	FRAP	AI_{50}	EI
TPC	1.000					
$TEAC_{DPPH}$	1.000	1.000				
$TEAC_{ABTS}$	1.000	1.000	1.000			
FRAP	1.000	1.000	1.000	1.000		
AI_{50}	−0.998	−0.998	−0.998	−0.997	1.000	
EI	0.696	0.696	0.694	0.681	−0.738	1.000

AI_{50} antioxidant index 50, *EI* electrochemical index, *FRAP* ferric reducing antioxidant power, *TEAC* Trolox equivalent antioxidant capacity, *TPC* total polyphenol content.

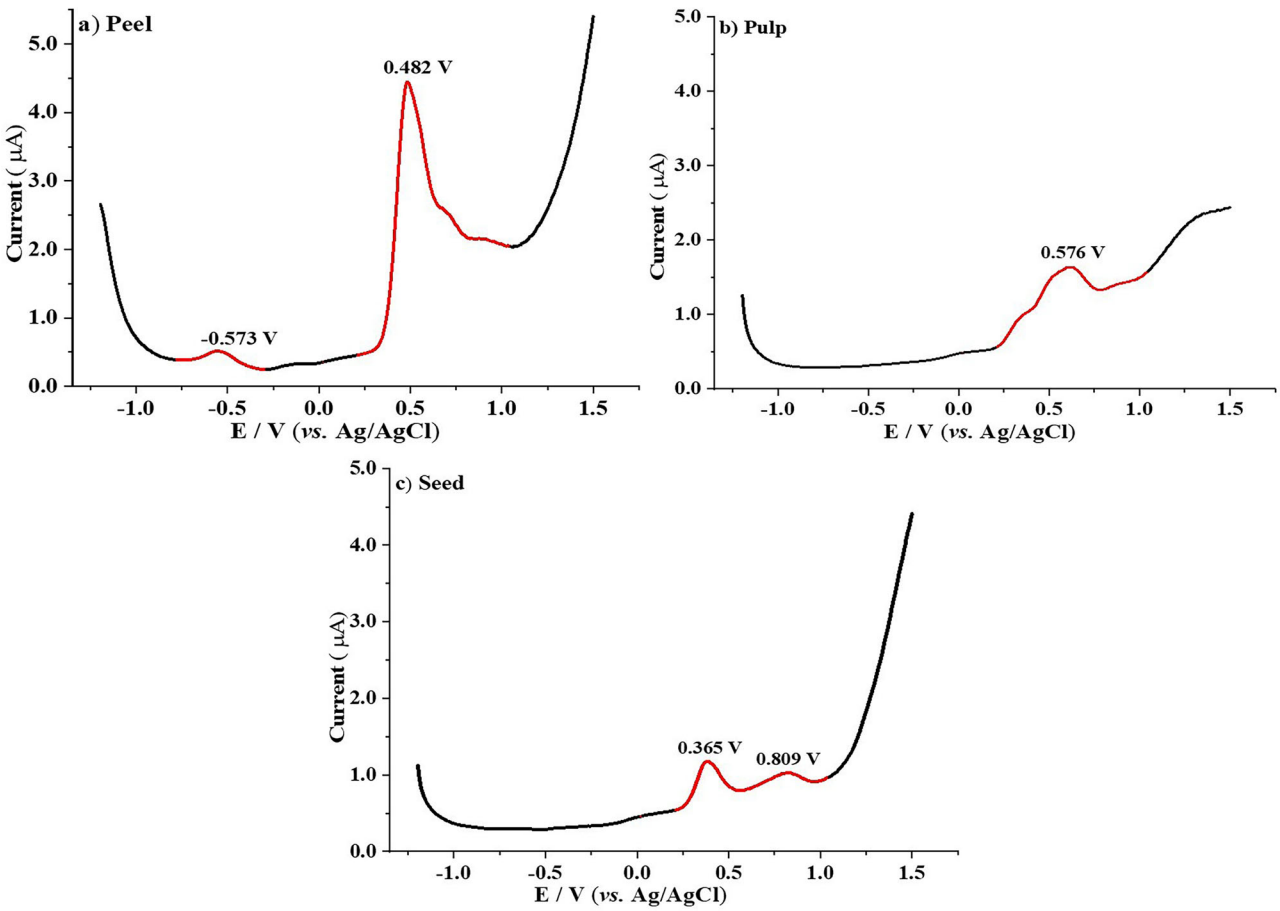

Fig. 5 | Differential pulse voltammograms of *P. cecropiifolia* Mart. extracts in acetate buffer (pH 4.5) at a scan rate of 17 mV s^{-1}. a Peel, **b** pulp, and **c** seed.

$R^2 = 1.000$; TPC-FRAP: $R^2 = 1.000$). Moreover, the correlation between spectroscopic and electrochemical AA assays also demonstrated a strong positive linear correlation, consistent with findings in previous studies[57,58]. AI_{50}, being inversely proportional to AA, showed a moderate negative linear correlation with TPC, $TEAC_{DPPH}$, $TEAC_{ABTS}$, FRAP, and EI values.

Effect of *P. cecropiifolia* Mart. extracts on cancer tumor cell proliferation

The inhibition of cell proliferation of hydroethanolic extracts from *P. cecropiifolia* Mart. (peel, pulp, and seed) on cell lines from cervix, colon, and breast tumors were also evaluated (Table 5). The results indicate that *P. cecropiifolia* extracts have selective cytotoxic activity on the cancer cell lines evaluated. The greatest activity was observed in the T47D cell line (ductal breast cancer), especially with the pulp extract. Low activity in the HeLa cell line suggests differences in the mechanisms of action or the sensitivity of the cells. While all 3 extracts were effective against T47D, the most active extract was pulp breast ductal cancer cells. This effect of pulp extract can be attributed to the presence of specialized metabolites, including procyanidin B2 and CGA. Previous clinical reports have shown that both procyanidin B2[59] and CGA[60] exhibit anti-proliferative effects against breast cancer cells. In addition, acceptable IC_{50} values for cytotoxicity (<100 μg mL^{-1}, according to NCI guidelines) have been reported for anthocyanin-rich extracts from the pericarp of *P. cecropiifolia* Mart. against HEp-2 (larynx), MKN-45 (gastric), and MCF-7 (breast) cancer cell lines[14].

Molecular docking and dynamics

In the search for anticancer agents, human cytochrome P450 1A1 (CYP 1A1) and human cytochrome P450 1B1 (CYP 1B1) drug target proteins have come into a focal point in research. CYP 1A1 plays an important role in the etiology of breast carcinoma as key regulator of 2-hydroxylation of estrogen[61,62]. Although its implication in cancer is not fully understood yet, reduction of CYP1A1 levels by inhibition or other means impairs proliferation in breast cancer cells[63]. CYP1B1, on the other hand, is considered as an "universal tumor antigen" involved the estrogen metabolism and the activation of procarcinogens[64–68]. Previous studies have reported that several synthetic small molecules inhibit CYP 1A1 and 1B1 therapeutic targets in cancer cells[69,70].

Molecular docking studies were conducted with eight majors naturally occurring compounds from *P. cecropiifolia* Mart extracts based on the total ion chromatogram as ligands and docked against CYP 1A1 and 1B1 (Table 6). The docking results showed that four compounds produced positive docking scores for either one or both human cytochrome P450 enzymes (CYP 1A1 and 1B1), suggesting they may not interact with the active sites of these enzymes. Upon examining the docking poses, procyanidin B2, neoolivil, mirificin, and carthamin were found to be too large to fit into the active sites of CYP 1A1 and 1B1, leading to several clashes with the enzymes. Consequently, these molecules were excluded as CYP targets.

Caffeic acid and epicatechin were the most active compounds with the highest binding energy towards CYP 1A1 and 1B1 underscoring their possible involvement in apoptotic signaling modulation. Previous docking studies have unveiled that epicatechin hold the potential to interact with specific targets, such as estrogen receptor beta, a potential target for triple-negative breast cancer[71]. These findings may support the promising synergistic activity of *P. cecropiifolia* Mart extracts against CYP 1A1 and 1B1 enzymes. In contrast, nortracheloside and istanbulin showed a higher affinity for CYP 1A1 than for CYP 1B1, suggesting selectivity toward this enzyme.

To understand the pharmacological activity of that most active compounds of *P. cecropiifolia* Mart extracts against CYP 1A1 and 1B1 enzymes, we focused our analysis on the dynamic stability of nortracheloside and epicatequin as ligands. According to the results from the simulations, the root-mean-square deviation (RMSD) values for the CYP 1A1 and 1B1 complexes with nortracheloside and epicatechin increased during the first few nanoseconds, gradually stabilizing toward the end of the simulation (Fig. 6a, b). The RMSD values fluctuated between 0.3 and 0.4 nm for all the studied systems, with slightly higher values for CYP 1B1 compared to CYP 1A1. This behavior was expected, as the protein undergoes conformational changes when a different ligand binds to the active site.

Analysis of the RMSD values for the different ligands revealed an RMSD value of 0.2 nm for the complex between nortracheloside and both CYPs (Fig. 7). In contrast, the RMSD value for epicatechin was below 0.1 nm (Fig. 7), indicating the structure maintained its conformation with minimal conformational changes throughout the simulation. The studied complexes exhibited stable dynamics, as RMSD values ≤ 0.2 nm confirm the accuracy of the docking method[72].

A hydrogen bond (HB) analysis showed that for CYP 1A1, nortracheloside (Fig. 8a) formed approximately two HBs throughout the simulation, while epicatechin (Fig. 8b) formed three HBs during most of the simulation. Both ligands were able to form up to six HBs at certain points during the simulation. At the end of the simulation, nortracheloside formed HBs with S122 and the main chain of N222, N223, F224, G316, and L496. Epicatechin formed HBs with N255 and the main chain of N223, F251, and L312.

In CYP 1B1, both ligands formed, on average, two HBs during the 200 ns simulation. At the end of the simulation, both compounds remained in the active site of the CYPs. Examining the HBs at the end of the simulation, nortracheloside (Fig. 9a) formed HBs with D333 and the main chain of S127. Interestingly, epicatechin (Fig. 9b) formed the same two HBs (S127, D333) and an additional HB with the main chain of D326 (Fig. 9b). The identified HBs networks can guide the exploration of novel potential drug targeting strategies.

Finally, the binding energy results (Table 7) indicate that all values were negative, suggesting possible interactions. When comparing the two compounds, nortracheloside appeared to bind more tightly than epicatechin to both CYPs. Furthermore, the binding energy was consistent with the

Table 5 | IC_{50} of *P. cecropiifolia* Mart. peel, pulp, and seed extracts on human cancer cell lines

	$IC_{50} \pm SE^a$			
	Human cancer cell lines			
Treatment μg mL^{-1}	Hela (Cervix)	RKO (Colon)	MCF-7 (Breast)	T47D (Breast)
Peel	>200	154.2 ± 2.6	153.9 ± 2.1	83.2 ± 4.3
Pulp	>200	194.1 ± 5.6	160.8 ± 5.1	45.2 ± 4.7
Seed	>200.	183.1 ± 2.1	124.2 ± 4.1	95 ± 2.1
Doxorubicin μM	5.0 ± 0.7	2.4 ± 0.1	2.4 ± 0.1	1.5 ± 0.2

[a]Standard error.

Table 6 | Docking results for the interaction of predominant compounds from *P. cecropiifolia* Mart. and human cytochrome P450 enzymes

Compound	CYP 1A1 score (kcal mol^{-1})	CYP 1B1 score (kcal mol^{-1})	Plant part
Caffeic acid	−10.7	−9.3	pulp
Procyanidin B2	4.1	9.4	pulp
Neoolivil	4	9.8	peel
Nortracheloside	−9.2	−4.1	peel
Mirificin	−4.4	0.2	peel
Istanbulin	−7	−4.8	peel
Epicatechin	−10	−10.3	peel
Carthamin	26.8	30.3	pulp

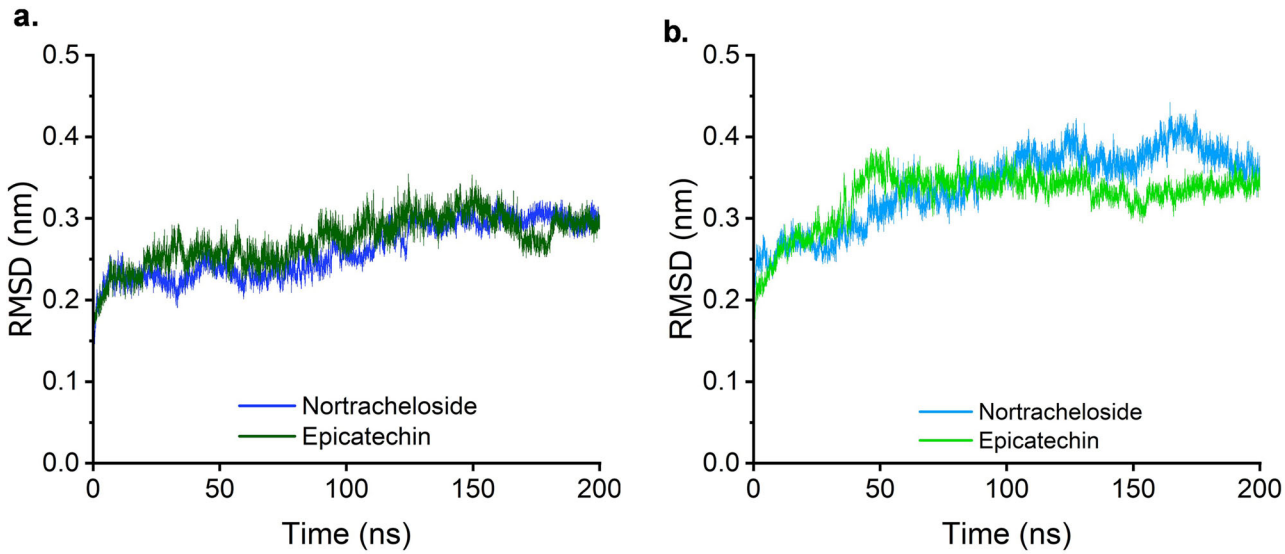

Fig. 6 | Root-mean-square deviation (RMSD) of the human cytochrome P450 enzymes in complex with nortracheloside and epicatechin during a 200 ns simulation. **a** CYP 1A1 and **b** CYP 1B1.

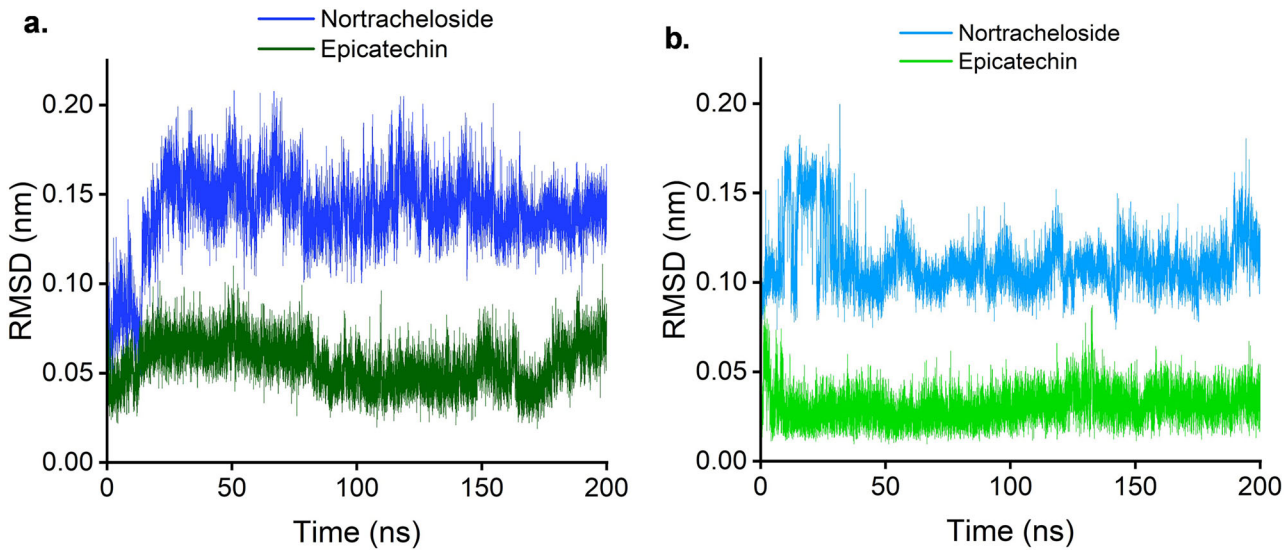

Fig. 7 | RMSD of the ligands in complex with the human cytochrome P450 enzymes during a 200 ns simulation. **a** CYP 1A1 and **b** CYP 1B1.

docking scores: for nortracheloside, the binding energy was 9.48 kcal mol^{-1} higher for CYP 1A1 than for CYP 1B1, implying a stronger inhibition of CYP 1A1. In contrast, epicatechin showed better docking scores and binding energy for CYP 1B1. The difference in energy (4.04 kcal mol^{-1}) was smaller than that for nortracheloside, which aligns with the observed docking score differences. In summary, these findings suggest that nortracheloside, epicatechin, along with other bioactive compounds in the extracts, hold promise as CYP 1A1 and 1B1 inhibitors.

In this study, the anticancer and antioxidant potential of hydroethanolic peel, pulp, and seed extracts of *P. cecropiifolia* Mart. were investigated. The findings of this study, which include UPLC-ESI-QTOF-MS and in silico analysis, are notable as they reveal that extracts of *P. cecropiifolia* Mart contain bioactive compounds of medicinal importance. Our findings revealed that pulp extracts of *P. cecropiifolia Mart.* shows moderate anticancer activity against breast ductal cancer cells. Furthermore, the results of an in silico study of the naturally occurring compounds *of P. cecropiifolia Mart* revealed that they can inhibit CYP 1A1 and 1B1 synergistically to prevent cancer. Nonetheless, the potential of these plant extracts and selected compounds implicated in treating cancer cell lines necessitates further pharmacological studies to validate the in vitro and in silico explorations. Finally, the current findings may provide the scientific base to conduct more studies on these plant extracts.

Methods

Chemicals, reagents, and cell lines

The following compounds were used in this study: DPPH, ferric chloride, ethanol, methanol, aluminum chloride, sodium nitrite, gallic acid, quercetin, tetrabutylammonium hexafluorophosphate, dimethyl sulfoxide, and tetrabutylammonium hexafluorophosphate (Bu_4NPF_6), all of which were extra-pure grade (>99%) and obtained from Sigma Aldrich (St. Darmstadt, Germany). Authentic phenolic compound standards used in the chromatographic analysis, including ascorbic acid (>99%) and *trans*-resveratrol (>99%), were also purchased from Sigma Aldrich. The chromatographic solvents used were of RP-HPLC-DAD grade. Ultrapure water (18 MΩ cm^{-1} conductivity) was prepared by purifying deionized water using a Thermo Scientific™ Barnstead™ GenPure™ water purification system.

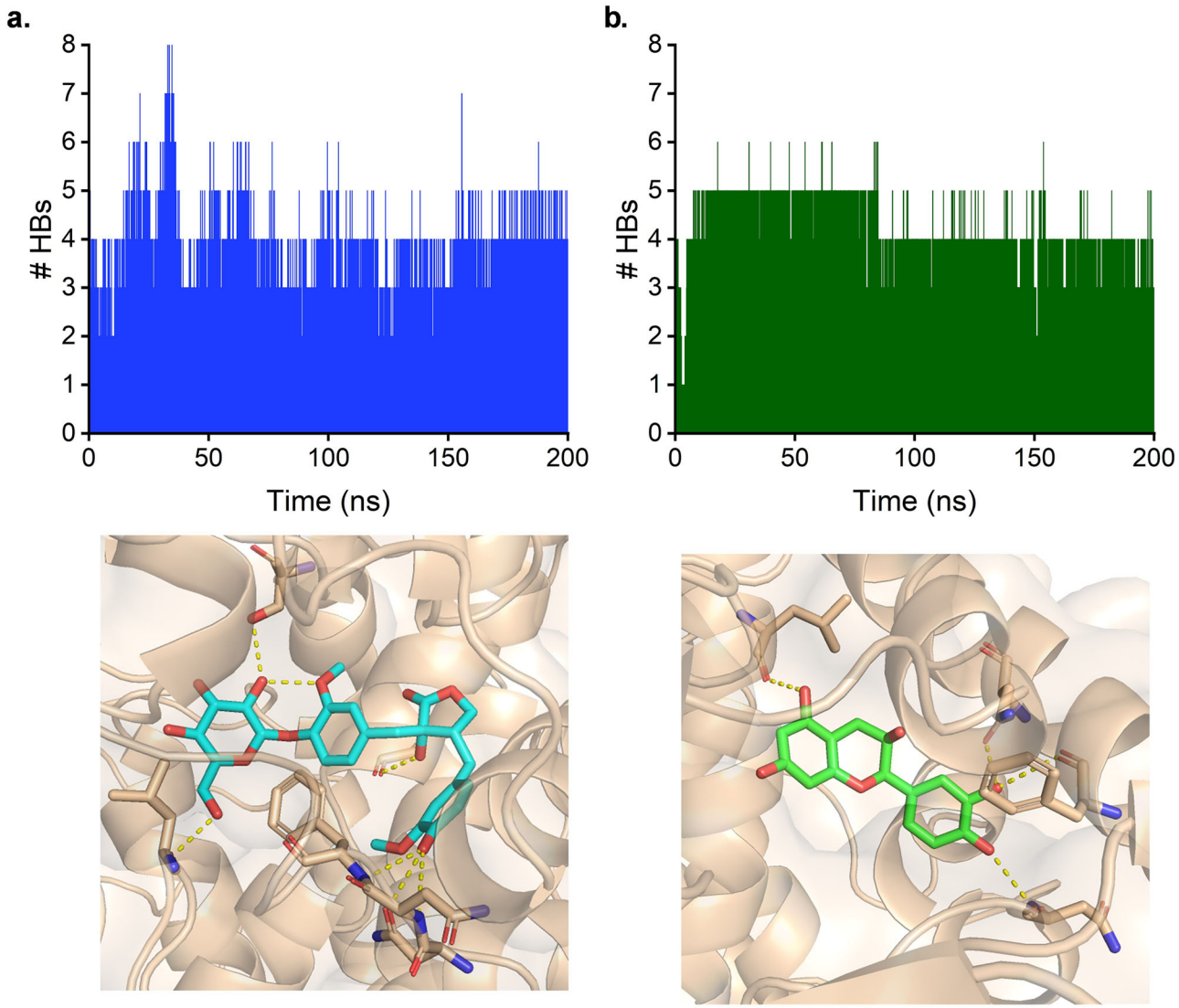

Fig. 8 | Hydrogen bond analysis of human cytochrome P450 1A1 in complex with ligands. a Nortracheloside and **b** epicatechin.

Cervix adenocarcinoma (Hela, CRM-CCL-2), colon (RKO, CRL-2577), breast cancer (MCF-7, HTB-22), and ductal breast cancer T-47D (HTB-133) were purchased from the American Type Culture Collection (Manassas, VA, USA). 3-(4,5-dimethylthiazol-2-yl)-5-(3-carboxymethoxyphenyl)-2-(4-sulfophenyl)-2H-tetrazolium, inner salt (MTS) was purchased from Promega, Madison, Wisconsin, USA.

Fruit collection and extraction

Samples of *P. cecropiifolia* Mart. were purchased from a local supplier in Parroquia Puerto Napo, Tena, Napo Province (1°02'19.2"S, 77°45'41.8"W) during the fruiting season (January–March 2022). The fruits were placed in sterile plastic bags and transported to the laboratory inside an icebox. For analysis, the peel, pulp, and seeds of the fruits were used. The samples were lyophilized using an SP Scientific-Genevac (BTP-9E LOVE) for 72 h until a constant weight was achieved. The lyophilized material was kept in an ultra-low freezer at −20 °C. Subsequently, the dried samples were ground into a fine powder using a laboratory mill. For extraction, powdered samples were soaked in a hydroethanolic solution (ethanol:H_2O, 40:60, v/v) at room temperature at a ratio of 1:10 (w/v). The resulting mixtures were then vortexed for 120 min under light-protected conditions (Supplementary Table 1). The supernatants were collected in 5 mL amber vials and stored in a refrigerator at −4 °C for further analysis[73].

Determination of TPC

The TPC of the extracts was evaluated following the method described by Kupina et al.[74]. Briefly, 100 µL of the extract was added to a test tube containing 40 µL of Folin–Ciocalteu reagent and 860 µL of water. The mixture was vigorously shaken and allowed to stand for 5 min. Subsequently, 100 µL of 7% (w/v) sodium carbonate and 900 µL of water were added. The resulting mixture was kept in the dark for 30 min. The absorbance was measured at 750 nm using a UV–vis spectrophotometer (Shimadzu UV-1280). TPC was expressed as milligrams of GAE per gram of dried extract (mg GAE g^{-1} d.w.).

Anthocyanin content

Anthocyanins were extracted using a 1:50 (m:v) ratio with 1.5 M HCl prepared in 85% ethanol. The extract was stored for 24 h at 4 °C[75]. After filtration, the absorbance was measured using a UV–vis spectrophotometer (UV-DR6000, Hach, Loveland, CO, USA). Anthocyanin content was calculated using the absorption coefficient of 982 (g 100 $mL^{-1})^{-1}$ cm^{-1} [75].

Total flavonoid content

The total flavonoid content of the hydroethanolic extracts was quantified using the aluminum chloride colorimetric assay as described by Chang et al.[76] The calibration curve was prepared by dissolving quercetin in methanol. In brief, 0.1 mL of the hydroethanolic extract or quercetin

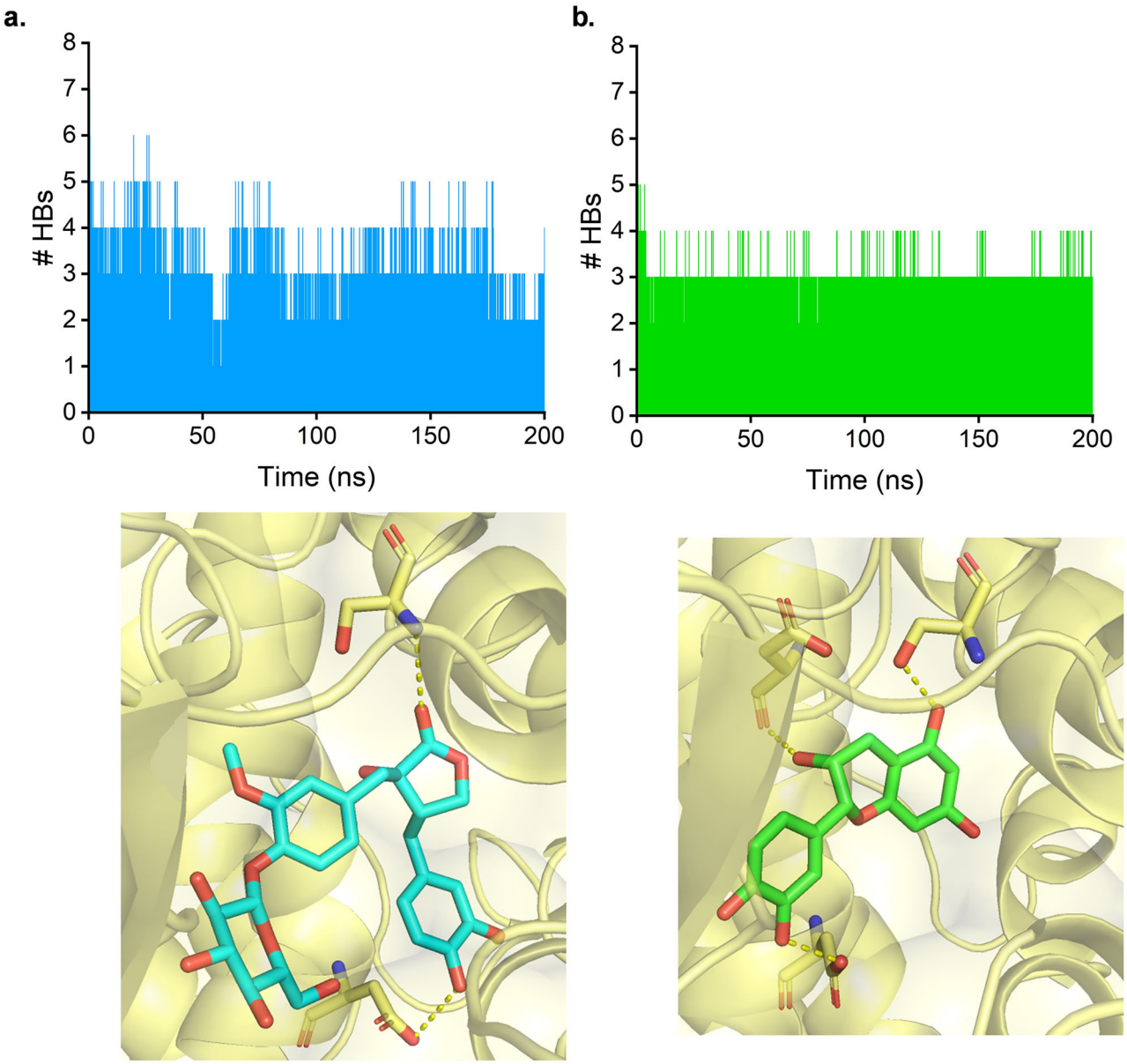

Fig. 9 | Hydrogen bond analysis of human cytochrome P450 1B1 in complex with ligands. a Nortracheloside and **b** epicatechin.

Table 7 | Van der Waals, electrostatic, SASA, and binding energy (in kcal mol^{-1}) of the compounds

Enzyme	Compound	Van der Waals energy	Electrostatic energy	SASA energy	Binding energy
CYP 1A1	Nortracheloside	−70.59	−9.82	−6.07	−34.57
	Epicatechin	−30.98	−15.99	−3.20	−16.21
CYP 1B1	Nortracheloside	−68.78	−16.88	−6.29	−25.09
	Epicatechin	−41.51	−13.95	−3.94	−20.25

CYP human cytochrome P450, *SASA* solvent-accessible surface area.

standard was mixed with 0.1 mL of 10% (w/v) aluminum chloride solution and 0.1 mL of 0.1 mM potassium acetate solution. The mixture was incubated for 30 min at room temperature. Absorbance was measured at 415 nm using a UV–vis spectrophotometer (UV-DR6000, Hach, Loveland, CO, USA). The results were expressed as milligrams of QE per gram of dried sample (mg QE g^{-1} d.w.).

Analysis of ascorbic acid and *trans*-resveratrol using HPLC

Ascorbic acid and *trans*-resveratrol were quantified using high-performance liquid chromatography (HPLC). The analysis was performed using a Hitachi LaChrom Elite® liquid chromatograph equipped with an autosampler and UV detector. A reverse-phase TC C-18 analytical column (150 mm × 4.6 mm, 5 µm particle size, Agilent, USA) was used for the separation.

Ascorbic acid was extracted using the method described by Chebrolu et al. with minor modifications[77]. An aqueous solution of 3% metaphosphoric acid (MPA) was used as the extraction solvent, and extractions were conducted at room temperature. Lyophilized fruit samples were mixed with the extraction solution at a 1:10 (w/v) ratio, vortex-stirred for 2 min, and sonicated for 2 min. The mixture was then centrifuged at 3000 rpm, and the resulting extracts were stored in sealed dark-glass vials at −4 °C prior to analysis. Separation of ascorbic acid was achieved via isocratic elution using a mobile phase of methanol and water (15:85 v/v) with a pH of 2.5 (adjusted with MPA). The flow rate was set at 1.2 mL min^{-1}, and UV detection was performed at 245 nm (Supplementary Fig. 1).

Trans-resveratrol extraction followed the method described by Sun et al.[78] with modifications. Briefly, 50 mg of lyophilized fruit was mixed with 2 mL of ethanol/water (70:30 v/v) as the extraction solvent. The mixture was then filtered through 0.45 µm PVDF filters. Separation was performed using isocratic elution of water/acetonitrile/acetic acid (70:29.9:0.1 v/v/v) at a flow rate of 1 mL min^{-1}. Detection was conducted at 306 nm, and the column oven temperature was set to 30 °C (Supplementary Fig. 2).

Analysis of *trans*-resveratrol via UPLC-QTOF-MS

Resveratrol was verified using UPLC-QTOF-MS (Waters Acquity UPLC Xevo G2-XS Q/TOF) with a scanning range of m/z 100 to 1200 Da in negative ionization mode. Separation was performed using an Acquity UPLC BEH C18 column (2.1 × 50 mm, 1.7 µm particle size, Waters, Milford, MA, USA) with a gradient mobile phase consisting of 0.01% formic acid in water (Solvent A) and 100% acetonitrile (Solvent B). Gradient elution conditions were as follows: 1% B (1 min), 1–20% B (10 min), 20–25% B (10 min), and 35–50% B (5 min), followed by column rebalancing. The flow rate was maintained at 0.25 mL min^{-1}. The optimized ESI parameters were: a capillary voltage of 0.5 kV, cone gas flow of 30 L h^{-1}, desolvation gas flow of 900 L h^{-1}, source temperature of 140 °C, desolvation temperature of 450 °C, sample cone voltage of 40 V, and source offset of 80 V. MS/MS analysis was conducted with a collision energy of 20 eV with the Acquity UPLC BEH C18 column. Data collection and analysis were carried out using UNIFI™ v1.8 software on the MassLynx NT 4.1 platform (Waters, Milford, MA, USA).

UPLC-QTOF-MS analysis

Metabolites in the hydroethanolic extract of *P. cecropiifolia* Mart. were identified using a UPLC-ESI-QTOF-MS system. The analysis was conducted in negative ionization mode with a scanning range of m/z 100–1200 Da. Chromatographic separation was achieved with an Acquity UPLC BEH C18 column (2.1 × 50 mm, 1.7 µm particle size, Waters, Milford, MA, USA). The LC mobile phase A consisted of 0.1% formic acid in water, while mobile phase B constituted 0.1% formic acid in acetonitrile. The gradient elution was as follows: 1% A (0–1 min), 1–20% A (10 min), 20–25% A (10 min), 25–35% A (5 min), 35–50% A (5 min), and 1% A (4 min). MS/MS parameters were as follows: a capillary voltage of 0.5 kV, source temperature of 140 °C, desolvation temperature of 450 °C, and sampling cone and source offset voltages of 40 and 80 V, respectively. The collision energy ramp was set to a low energy of 6 eV and a high energy range of 20–30 eV. Mass spectral data collection and analysis followed the previously described methodology for UPLC-ESI-QTOF-MS/MS analysis of *trans*-resveratrol.

DPPH free radical scavenging activity

The DPPH radical scavenging capacity was carried out in triplicate following the method of Gulati et al.[79] with minor modifications. Six different concentrations of the extracts were mixed with 0.6 µM DPPH prepared in ethanol (96% w/w). Each reaction consisted of 50 µL of DPPH working solution, 100 µL of sample dilutions (ethanol served as the blank), and 100 µL of ethanol. The fruit extracts were prepared in test tubes containing ethanol to give 1001.5 to 4280.0, 6011.3 to 29040.0, and 20.2 to 199.9 µg mL^{-1} solutions for peel, pulp, and seed, respectively. The mixtures were incubated in a dark room on an orbital shaker (Orbit™ LS Low-Speed Laboratory Shaker, Labnet) at 60 rpm. The absorbance of each concentration was measured at 517 nm using a spectrophotometer (Promega, Glomax Discover System). Trolox was used as the positive control. The percent radical scavenging activity of the extracts was calculated using the following Eq. (1):

$$\text{DPPH radical scavenging activity}(\%) = \frac{(\text{Abs control} - \text{Abs sample}) * 100}{\text{Abs control}} \quad (1)$$

where Abs control is the absorbance of DPPH + ethanol and Abs sample is the absorbance of DPPH radical + sample (sample or standard). The IC_{50} values can be calculated with GraphPad Prism® software using a nonlinear regression as follows, Eq. (2):

$$Y = \frac{100}{\left(1 + 10^{((\text{LogIC50} - X) * \text{HillSlope})}\right)} \quad (2)$$

The results were expressed as TEAC, was estimated using the equation below[80], Eq. (3):

$$TEAC = \frac{IC_{50} of\ Trolox\left(\frac{ug}{L}\right)}{IC_{50} of\ sample\left(\frac{ug}{L}\right)} \quad (3)$$

ABTS free radical scavenging activity

The ABTS radical cation decolorization assay was performed following the method of Re et al.[81] Briefly, a solution of 7.07 mM ABTS was prepared by mixing it with 2.45 mM potassium persulfate to produce the ABTS radical cation. The mixture was incubated in the dark at room temperature for 16 h. The resulting ABTS radical solution was diluted with ethanol (96% w/w) to achieve an absorbance of 0.7 at 734 nm. A reaction mixture was prepared by combining 2850 µL of the ABTS reagent with 150 µL of either standard (Trolox) or extract solutions at concentrations of 800.0 to 448.8, 1106.2 to 29040.0, and 21.0 to 116.5 µg mL^{-1} for peel, pulp, and seed extracts, respectively. Trolox was used as a positive control, with a concentration range of 10 to 320 µM. All measurements were carried out at least three times. TEAC was calculated using the same equation as that for the DPPH free radical scavenging activity.

FRAP assay

The FRAP of the hydroethanolic extracts was assessed according to the method outlined by Benzie and Strain[82]. Briefly, the reaction mixture was prepared by mixing 300 µL of FRAP reagent, 30 µL of distilled water, and 10 µL of sample in a 96-well microtiter plate reader. The mixture was incubated at 37 °C for 4 min in the dark, and the absorbance was measured at 600 nm using a Promega Glomax Discover System spectrophotometer. Antioxidant capacity was expressed as µmol Fe^{2+} g^{-1} d.w.

Antioxidant capacity assessment via CV

Antioxidant capacity was evaluated by analyzing changes in the current of the superoxide anion radical in the presence of increasing concentrations of antioxidants (0.51 to 2.57 mg mL^{-1}). The AI_{50} was determined from the plot of the dimensionless parameter $((Ip_a^0\text{-}Ip_a^s)/Ip_a^0)$ *vs.* antioxidant concentration, where, Ip_a^0 is the peak current in the oxidative scan without the antioxidant in the medium, and Ip_a^s is the peak current with the antioxidant. The AI_{50} value represents the concentration of an antioxidant necessary to decrease the anodic peak current by 50%. In this assay, the lower the AI_{50} value, the higher the antioxidant potency, signifying greater capacity to scavenge superoxide anion radicals[83,84].

CV measurements were performed according to Barrietos et al.[85] using a computer-controlled electrochemical system (CH Instruments) equipped with a standard three-electrode cell assembly. A glassy carbon electrode (3 mm in diameter) served as the working electrode, Ag/AgCl as the reference electrode, and a graphite rod as the counter electrode. The working solution consisted of 0.05 M tetrabutylammonium hexafluorophosphate in dimethylformamide. Before each measurement, the working electrode was polished with alumina of decreasing granulometry (0.3, 0.1, and 0.05 µm), rinsed with deionized water, sonicated for 1 min, rinsed with acetone, and dried with air. The cell was saturated with O_2 by bubbling air through the solution for 1 min, generating the superoxide anion radical ($O_2^{\bullet-}$) through the one-electron reduction of molecular oxygen. Voltammetric signals were recorded at room temperature using a scan rate of 0.1 V s^{-1} and potential window from −0.2 to −1.0 V (*vs.* Ag/AgCl).

Antioxidant capacity assessed using DPV

The antioxidant capacity of the extracts was further evaluated using the electrochemical index (EI)calculated through DPV as per Eq. (4)[86]:

$$EI = \frac{I_{pa,1}}{E_{pa,1}} + \frac{I_{pa,2}}{E_{pa,2}} + \frac{I_{pa,3}}{E_{pa,3}} + \ldots + \frac{I_{pa,n}}{E_{pa,n}} \quad (4)$$

where i_{pa} represents the current value and E_{pa} the potential value for each major anodic peak in the DPV voltammogram. DPV measurements were carried out using the same electrochemical setup as described previously. The electrolytic solution consisted of 0.1 M acetate buffer (pH = 5). Prior to each measurement, nitrogen purging was performed for 30 s. DPV was conducted in a potential window of −1.2 to 1.5 V (*vs.* Ag/AgCl) and a scan rate of 17 mV s^{-1}.

Antiproliferation assay

Cells Hela, RKO, MCF7 y T47D were cultured in DMEM and T-47D in RPMI. Mediums were supplemented with 100 units mL^{-1} penicillin G, 100 µg mL^{-1} streptomycin, 0.25 µg mL^{-1} amphotericin B, 2 mM L-glutamine, and 10% fetal bovine serum. The cells were grown in a humidified incubator (37 °C, 5% CO_2). Cultures were maintained in a humidified incubator at 37 °C with 5% CO_2. Cell viability was assessed using the MTS assay, which measures mitochondrial respiratory activity as an indicator of inhibited growth of human cancer cell lines. A total of 3×10^3 cells were seeded per well in a 96-well plate. After 24 h, the cells were treated with *P. cecropiifolia* Mart. extracts (peel, pulp, and seed) for an additional 24 h. for 5 different concentrations, ranging from 2 to 200. DMSO was used as the vehicle at a final concentration of 0.1% v/v, serving as the negative control. Doxrubicin was used as a positive control in ranges of 0.1 to 10. Each concentration was performed three times in triplicate. Cells were incubated with the treatments for 48 h. At 44 h, MTS solution (5 mg mL^{-1}) was added, and cells were further incubated for 4 h at 37 °C. Absorbance was measured at 570 nm with a reference wavelength of 650 nm. The percentage of inhibition was calculated using the following formula: viability (%) = (absorbance of treated cells/absorbance of control cells) × 100%.

Molecular docking and dynamics

To further investigate the anticancer activity of *P. cecropiifolia* Mart., molecular docking and molecular dynamics simulations were performed. The eight most predominant compounds identified from the chemical profile—three from the pulp and five from the peel—were selected for analysis, as cytotoxicity effects are likely attributed to compounds present in greater quantities. For the receptor, the X-ray crystal structures of human cytochrome P450 1A1 (CYP 1A1)[87] and human cytochrome P450 1B1 (CYP 1B1)[88] were selected as possible targets for cytotoxicity based on previous studies[89]. Docking studies were performed with an exhaustiveness parameter of 32, 1 Å spacing, full ligand flexibility, and a calculation box focused on the active sites of the selected CYPs. Structures were prepared using AutoDockTools[90], and calculations run using AutoDock Vina[91]. The results of docking calculations were used as input for the molecular dynamic simulation. The topology of the enzymes was built using the AMBER99SB-ILDN force field[92], while ligand topology was generated using the ACPYPE server[93] with the Generalized Amber Force Field[94]. The ligand–enzyme complexes were solvated using the three-point water model (TIP3P) and neutralized with Cl^- or Na^+ ions as needed. The system was energy-minimized and equilibrated at 300 K for 100 ps following NVT and NPT protocols[95]. Simulations were run at 300 K and 1 bar for 200 ns using GROMACS 2019[96]. Free binding energy was calculated from the trajectory data using the g_mmpbsa tool, applying the Molecular Mechanics Poisson–Boltzmann Surface Area method[97].

Statistical analysis

All experiments were performed in triplicate, and the results were expressed as mean ± standard deviation. We conducted a one-way analysis of the variance (ANOVA) followed by Tukey's test ($p > 0.05$) to identify statistical differences using R v.3.6.2 (R development). The relationships among DPPH, ABTS, FRAP, EI, AI_{50}, and TPC were evaluated using correlation analysis. IC_{50} values were calculated via nonlinear regression analysis using GraphPad Prism v. 10.4.1 (GraphPad Software Inc., USA).

Data availability

Data is provided within the manuscript or supplementary information files.

Code availability

No applicable.

Abbreviations

UPLC-ESI-QTOF-MS	ultra-performance liquid chromatography with electrospray ionization quadrupole time-of-flight mass spectrometry
AA	antioxidant activity
DPPH	2,2-diphenyl-1-picrylhidrazyl radical
ABTS	2,2'-azino-bis(3-ethylbenzothiazoline-6-sulfonic acid)
FRAP	ferric reducing antioxidant power
TEAC	Trolox equivalent antioxidant capacity
AI_{50}	antioxidant index 50
EI	electrochemical index
CV	cyclic voltammetry
DPV	differential pulse voltammetry
TPC	total phenolic content
GAE	gallic acid equivalent
TFC	Total flavonoid content
TAC	Total anthocyanin content
QE	quercetin equivalent
CGA	chlorogenic acid
MPA	metaphosphoric acid
MTS	3-(4,5-dimethylthiazol-2-yl)-5-(3-carboxymethoxyphenyl)-2-(4-sulfophenyl)-2h-tetrazolium, inner salt
RMSD	root-mean-square deviation
CYP 1A1	Cytochrome P450 1A1
CYP 1B1	Cytochrome P450 1B1

Received: 29 December 2024; Accepted: 23 June 2025;
Published online: 14 August 2025

References

1. Karges, J. Encapsulation of Ru(II) polypyridine complexes for tumor-targeted anticancer therapy. *BME Front.* **4**, 0024 (2023).
2. Mazurakova, A. Anti-breast cancer effects of phytochemicals: primary, secondary, and tertiary care. *EPMA J.* **13**, 315–354 (2022).
3. Liang, X. et al. Metal-organic framework-based photodynamic combined immunotherapy against the distant development of triple-negative breast cancer. *Biomater. Res.* **27**, 120 (2023).
4. Park, H. S. et al. Bifunctional tumor-targeted bioprobe for Phothotheranosis. *Biomater. Res.* **28**, 0002 (2024).
5. Wu, H. et al. Ginsenoside Rg3 nanoparticles with permeation enhancing based chitosan derivatives were encapsulated with doxorubicin by thermosensitive hydrogel and anti-cancer evaluation of peritumoral hydrogel injection combined with PD-L1 antibody. *Biomater. Res.* **26**, 77 (2022).
6. Gahtori, R. et al. Anticancer plant-derivatives: deciphering their oncopreventive and therapeutic potential in molecular terms. *Future J. Pharm. Sci.* **9**, 14 (2023).
7. Howes, M. R. et al. Molecules from nature: Reconciling biodiversity conservation and global healthcare imperatives for sustainable use of medicinal plants and fungi. *Plants People Planet* **2**, 463–481 (2020).
8. Garagounis, C., Delkis, N. & Papadopoulou, K. K. Unraveling the roles of plant specialized metabolites: using synthetic biology to design molecular biosensors. *N. Phytol.* **231**, 1338–1352 (2021).

9. Messinese, E. et al. By-products as a sustainable source of bioactive compounds for potential application in the field of food and new materials for packaging development. *Food Bioprocess Technol*. https://doi.org/10.1007/s11947-023-03158-2 (2023).
10. Silva, D. H. S., Castro-Gamboa, I. & Bolzani, V. D. S. Plant diversity from Brazilian Cerrado and Atlantic forest as a tool for prospecting potential therapeutic drugs. In *Comprehensive Natural Products II* 95–133 (Elsevier, 2010). https://doi.org/10.1016/B978-008045382-8.00061-7.
11. Maldonado, Y. E. A new essential oil from the native Ecuadorian species Steiractinia sodiroi (Hieron.) S.F. Blake (Asteraceae): chemical and enantioselective analyses. *Sci. Rep.* **13**, 17180 (2023).
12. Ortiz, O. O., Rivera-Mondragón, A., Pieters, L., Foubert, K. & Caballero-George, C. Cecropia telenitida Cuatrec. (Urticaceae: Cecropieae): Phytochemical diversity, chemophenetic implications and new records from Central America. *Biochem. Syst. Ecol.* **86**, 103935 (2019).
13. Kasangana, P., Haddad, P. & Stevanovic, T. Study of polyphenol content and antioxidant capacity of Myrianthus Arboreus (Cecropiaceae) root bark extracts. *Antioxidants* **4**, 410–426 (2015).
14. Barrios, J. et al. Chemical analysis and screening as anticancer agent of anthocyanin-rich extract from Uva Caimarona (Pourouma cecropiifolia Mart.) Fruit. *J. Agric. Food Chem.* **58**, 2100–2110 (2010).
15. Yánez, P. Distribución geográfica y aspectos etnobotánicos de tres especies delgénero pourouma ("uva de monte"), Cecropiaceae, en la región amazónica de Ecuador. *Rev. Forest. Venez.* **43**, 103–109 (1999).
16. Lopes-Lutz, D., Dettmann, J., Nimalaratne, C. & Schieber, A. Characterization and quantification of polyphenols in Amazon Grape (Pourouma cecropiifolia Martius). *Molecules* **15**, 8543–8552 (2010).
17. Lim, T. K. Pourouma cecropiifolia. In *Edible Medicinal And Non-Medicinal Plants* 446–449 (Springer Netherlands, Dordrecht, 2013). https://doi.org/10.1007/978-94-007-5628-1_50.
18. Fagbemi, K. O. et al. Bioactive compounds, antibacterial and antioxidant activities of methanol extract of Tamarindus indica Linn. *Sci. Rep.* **12**, 9432 (2022).
19. Osman, A. et al. Dietary polyphenols drive dose-dependent behavioral and molecular alterations to repeated morphine. *Sci. Rep.* **13**, 12223 (2023).
20. Ordoñez, E., Leon-Arevalo, A., Rivera-Rojas, H. & Vargas, E. Quantification of total polyphenols and antioxidant capacity in skins and seeds from cacao (Theobroma cacao L.), tuna (Opuntia ficus indica Mill), grape (Vitis Vinífera) and uvilla (Pourouma cecropiifolia). *Sci. Agropecu.* **10**, 175–183 (2019).
21. Ebata, K. T. Vitamin C induces specific demethylation of H3K9me2 in mouse embryonic stem cells via Kdm3a/b. *Epigenetics & chromatin.* **10**, 1–12 (2017).
22. Carr, A. C. & Frei, B. Toward a new recommended dietary allowance for vitamin C based on antioxidant and health effects in humans. *Am. J. Clin. Nutr.* **69**, 1086–1107 (1999).
23. Rao, A. et al. TET family dioxygenases and the TET activator vitamin C in immune responses and cancer. *Blood* **136**, 1394–1401 (2020).
24. Gustafson, C. B. et al. Epigenetic reprogramming of melanoma cells by vitamin C treatment. *Clin. Epigenet.***7**, 51 (2015).
25. Agathocleous, M. et al. Ascorbate regulates haematopoietic stem cell function and leukaemogenesis. *Nature* **549**, 476–481 (2017).
26. Guan, Y. et al. Context dependent effects of ascorbic acid treatment in TET2 mutant myeloid neoplasia. *Commun. Biol.* **3**, 493 (2020).
27. Abreu-Naranjo, R. et al. Bioactive compounds, phenolic profile, antioxidant capacity and effectiveness against lipid peroxidation of cell membranes of Mauritia flexuosa L. fruit extracts from three biomes in the Ecuadorian Amazon. *Heliyon* **6**, e05211 (2020).
28. Bhattacharya, S. Therapeutic role of resveratrol against hepatocellular carcinoma: A review on its molecular mechanisms of action. *Pharmacol. Res.* **6**, 100233 (2023).
29. Okudaira, N., Ishizaka, Y. & Tamamori-Adachi, M. Resveratrol blocks retrotransposition of LINE-1 through PPAR α and sirtuin-6. *Sci. Rep.* **12**, 7772 (2022).
30. Wei, J., et al. Exploring the biomolecular mechanism of resveratrol in the treatment of nephrotic syndrome based on network pharmacology. *Pharmacol. Res. Chin. Med.* **3**, 100114 (2022).
31. Zhang, L.-X. et al. Resveratrol (RV): A pharmacological review and call for further research. *Biomed. Pharmacother.* **143**, 112164 (2021).
32. Hou, X., Rooklin, D., Fang, H. & Zhang, Y. Resveratrol serves as a protein-substrate interaction stabilizer in human SIRT1 activation. *Sci. Rep.* **6**, 38186 (2016).
33. Craveiro, M. et al. Resveratrol stimulates the metabolic reprogramming of human $CD4^+$ T cells to enhance effector function. *Sci. Signal.* **10**, eaal3024 (2017).
34. Shrikanta, A., Kumar, A. & Govindaswamy, V. Resveratrol content and antioxidant properties of underutilized fruits. *J. Food Sci. Technol.* **52**, 383–390 (2015).
35. Fraisse, D., Heitz, A., Carnat, A., Carnat, A.-P. & Lamaison, J.-L. Quercetin 3-arabinopyranoside, a major flavonoid compound from Alchemilla xanthochlora. *Fitoterapia* **71**, 463–464 (2000).
36. Falchero, L. et al. Essential oil composition of lady's mantle (*Alchemilla xanthochlora* Rothm.) growing wild in Alpine pastures. *Nat. Prod. Res.* **23**, 1367–1372 (2009).
37. Fan, P., Terrier, L., Hay, A.-E., Marston, A. & Hostettmann, K. Antioxidant and enzyme inhibition activities and chemical profiles of Polygonum sachalinensis F.Schmidt ex Maxim (Polygonaceae). *Fitoterapia* **81**, 124–131 (2010).
38. Huber, R. et al. In vitro antiallergic effects of aqueous fermented preparations from *Citrus* and *Cydonia* fruits. *Planta Med* **78**, 334–340 (2012).
39. Noshita, T., Funayama, S., Hirakawa, T., Kidachi, Y. & Ryoyama, K. Machilin G and four neolignans from young fruits of *Magnolia denudata* show various degrees of inhibitory activity on Nitric Oxide (NO) production. *Biosci. Biotechnol. Biochem.* **72**, 2775–2778 (2008).
40. Liu, X.-T. et al. Active components with inhibitory activities on IFN-γ/STAT1 and IL-6/STAT3 signaling pathways from Caulis Trachelospermi. *Molecules* **19**, 11560–11571 (2014).
41. Masuda, I. et al. Apple procyanidins promote mitochondrial biogenesis and proteoglycan biosynthesis in chondrocytes. *Sci. Rep.* **8**, 7229 (2018).
42. Forino, M. et al. 1S,3R,4S,5R)5-O-Caffeoylquinic acid: Isolation, stereo-structure characterization and biological activity. *Food. Chem.* **178**, 306–310 (2015).
43. Fischer, H. O. L. & Dangschat, G. Konstitution der Chlorogensäure (3. Mitteil. über Chinasäure Derivate). *Ber. Dtsch. Chem. Ges. B Ser.* **65**, 1037–1040 (1932).
44. Gupta, A., Atanasov, A. G., Li, Y., Kumar, N. & Bishayee, A. Chlorogenic acid for cancer prevention and therapy: Current status on efficacy and mechanisms of action. *Pharmacol. Res.* **186**, 106505 (2022).
45. Wang, X., Qin, L., Zhou, J., Li, Y. & Fan, X. A novel design to screen chlorogenic acid-producing microbial strains from the environment. *Sci. Rep.* **8**, 14756 (2018).
46. Zuo, J., Tang, W. & Xu, Y. Anti-Hepatitis B virus activity of chlorogenic acid and its related compounds. in *Coffee in Health and Disease Prevention* 607–613 (Elsevier, 2015). https://doi.org/10.1016/B978-0-12-409517-5.00068-1.
47. Chai, X. et al. Chlorogenic acid protects against myocardial ischemia–reperfusion injury in mice by inhibiting Lnc Neat1/NLRP3 inflammasome-mediated pyroptosis. *Sci. Rep.* **13**, 17803 (2023).
48. Fan, X., Jiao, W., Wang, X., Cao, J. & Jiang, W. Polyphenol composition and antioxidant capacity in pulp and peel of apricot fruits of various varieties and maturity stages at harvest. *Int. J. Food Sci. Technol.* **53**, 327–336 (2018).

49. Biswas, A. et al. Phytochemical content and antioxidant activity of different anatomical parts of Corchorus olitorius and C. capsularis during different phenological stages. *Heliyon* **9**, e16494 (2023).
50. Kumar, N. & Goel, N. Phenolic acids: Natural versatile molecules with promising therapeutic applications. *Biotechnol. Rep.* **24**, e00370 (2019).
51. Kabtni, S. et al. Influence of climate variation on phenolic composition and antioxidant capacity of Medicago minima populations. *Sci. Rep.* **10**, 8293 (2020).
52. Keffous, F. et al. Determination of the antioxidant activity of *Limoniastrum feei* aqueous extract by chemical and electrochemical methods. *Cogent Chem.* **2**, 1186141 (2016).
53. Muhammad, H. et al. Electrochemical behavior of superoxide anion radical towards quinones: a mechanistic approach. *Res. Chem. Intermed.* **44**, 6387–6400 (2018).
54. Sochor, J. et al. Electrochemistry as a tool for studying antioxidant properties. *Int. J. Electrochem. Sci.* **8**, 8464–8489 (2013).
55. Iloki-Assanga, S. B. et al. Solvent effects on phytochemical constituent profiles and antioxidant activities, using four different extraction formulations for analysis of Bucida buceras L. and Phoradendron californicum. *BMC Res. Notes* **8**, 396 (2015).
56. Aksoy, L., Kolay, E., Ağılönü, Y., Aslan, Z. & Kargıoğlu, M. Free radical scavenging activity, total phenolic content, total antioxidant status, and total oxidant status of endemic Thermopsis turcica. *Saudi J. Biol. Sci.* **20**, 235–239 (2013).
57. Ruiz-Caro, P. et al. An electrochemical alternative for evaluating the antioxidant capacity in walnut kernel extracts. *Food Chem.* **393**, 133417 (2022).
58. Osorio-Valencia, A. I. et al. Evaluation of antioxidant capacity in different food matrices through differential pulse voltammetry and its correlation with spectrophotometric methods. *J. Appl. Electrochem*. (2023) https://doi.org/10.1007/s10800-023-01933-9.
59. Gouvêa, CibeleM, C. P. & Avelar, M. Procyanidin B2 cytotoxicity to MCF-7 human breast adenocarcinoma cells. *Indian J. Pharm. Sci.* **74**, 351 (2012).
60. Changizi, Z., Moslehi, A., Rohani, A. & Eidi, A. Chlorogenic acid inhibits growth of 4T1 breast cancer cells through involvement in Bax/Bcl2 pathway. *J. Cancer Res. Ther.* **16**, 1435 (2020).
61. Shin, A. et al. Cytochrome P450 1A1 (CYP1A1) polymorphisms and breast cancer risk in Korean women. *Exp. Mol. Med.* **39**, 361–366 (2007).
62. Mukherjee, G., Nandekar, P. P. & Wade, R. C. An electron transfer competent structural ensemble of membrane-bound cytochrome P450 1A1 and cytochrome P450 oxidoreductase. *Commun. Biol.* **4**, 55 (2021).
63. Rodriguez, M. & Potter, D. A. CYP1A1 regulates breast cancer proliferation and survival. *Mol. Cancer Res.* **11**, 780–792 (2013).
64. Gribben, J. G. et al. Unexpected association between induction of immunity to the universal tumor antigen CYP1B1 and response to next therapy. *Clin. Cancer Res.* **11**, 4430–4436 (2005).
65. Li, F., Zhu, W. & Gonzalez, F. J. Potential role of CYP1B1 in the development and treatment of metabolic diseases. *Pharmacol. Ther.* **178**, 18–30 (2017).
66. D'Uva, G., Baci, D., Albini, A. & Noonan, D. M. Cancer chemoprevention revisited: Cytochrome P450 family 1B1 as a target in the tumor and the microenvironment. *Cancer Treat. Rev.* **63**, 1–18 (2018).
67. Chen, C. et al. CYP1B1 inhibits ferroptosis and induces anti-PD-1 resistance by degrading ACSL4 in colorectal cancer. *Cell Death Dis.* **14**, 271 (2023).
68. Chun, Y. & Kim, S. Discovery of cytochrome P450 1B1 inhibitors as new promising anti-cancer agents. *Med. Res. Rev.* **23**, 657–668 (2003).
69. Dutour, R. & Poirier, D. Inhibitors of cytochrome P450 (CYP) 1B1. *Eur. J. Med. Chem.* **135**, 296–306 (2017).
70. Liu, J., Sridhar, J. & Foroozesh, M. Cytochrome P450 Family 1 inhibitors and structure-activity relationships. *Molecules* **18**, 14470–14495 (2013).
71. Rammali, S. et al. In vitro and computational investigation of antioxidant and anticancer properties of Streptomyces coeruleofuscus SCJ extract on MDA-MB-468 triple-negative breast cancer cells. *Sci. Rep.* **14**, 25251 (2024).
72. Shahab, M. et al. Targeting human progesterone receptor (PR), through pharmacophore-based screening and molecular simulation revealed potent inhibitors against breast cancer. *Sci. Rep.* **14**, 6768 (2024).
73. Stafussa, A. P. et al. Bioactive compounds of 44 traditional and exotic Brazilian fruit pulps: phenolic compounds and antioxidant activity. *Int. J. Food Prop.* **21**, 106–118 (2018).
74. Kupina, S., Fields, C., Roman, M. C. & Brunelle, S. L. Determination of Total Phenolic Content Using the Folin-C Assay: Single-Laboratory Validation, First Action 2017.13. *J. AOAC Int.* **101**, 1466–1472 (2018).
75. Silva, L. M. R. D. et al. Quantification of bioactive compounds in pulps and by-products of tropical fruits from Brazil. *Food Chem.* **143**, 398–404 (2014).
76. Tuah, B., Asante, M., Asare, G. & Doku, D. In vitro antioxidant activity in seven selected local Ghanaian spices and an artificial spice, Shrimp Cube. *World J. Nutr. Health* **5**, 46–52 (2017).
77. Chebrolu, K. K., Jayaprakasha, G. K., Yoo, K. S., Jifon, J. L. & Patil, B. S. An improved sample preparation method for quantification of ascorbic acid and dehydroascorbic acid by HPLC. *LWT* **47**, 443–449 (2012).
78. Sun, H., Lin, Q., Wei, W. & Qin, G. Ultrasound-assisted extraction of resveratrol from grape leaves and its purification on mesoporous carbon. *Food Sci. Biotechnol.* **27**, 1353–1359 (2018).
79. Gulati, V., Harding, I. H. & Palombo, E. A. Enzyme inhibitory and antioxidant activities of traditional medicinal plants: Potential application in the management of hyperglycemia. *BMC Complement. Altern. Med*. **12**, 1–9 (2012).
80. Xiao, F., Xu, T., Lu, B. & Liu, R. Guidelines for antioxidant assays for food components. *Food Front.* **1**, 60–69 (2020).
81. Re, R. et al. Antioxidant activity applying an improved ABTS radical cation decolorization assay. *Free Radic. Biol. Med.* **26**, 1231–1237 (1999).
82. Benzie, I. F. F. & Strain, J. J. The Ferric Reducing Ability of Plasma (FRAP) as a measure of "Antioxidant Power": The FRAP assay. *Anal. Biochem.* **239**, 70–76 (1996).
83. Herrera-Marín, P. et al. Green synthesis of silver nanoparticles using aqueous extract of the leaves of fine aroma cocoa Theobroma cacao linneu (Malvaceae): Optimization by electrochemical techniques. *Electrochim. Acta* **447**, 142122 (2023).
84. Pérez-Cruz, K. et al. Synthesis and antioxidant study of new polyphenolic hybrid-coumarins. *Arab. J. Chem.* **11**, 525–537 (2018).
85. Barrientos, C., Navarrete-Encina, P. & Squella, J. A. Electrochemistry and reactivity against superoxide anion radicals of Hydroxycoumarins and its derivatives. *J. Electrochem. Soc.* **167**, 165502 (2020).
86. Kinyua Muthuri, L., Nagy, L. & Nagy, G. Chronopotentiometric method for assessing antioxidant activity: A reagentless measuring technique. *Electrochem. Commun.* **122**, 106907 (2021).
87. Walsh, A. A., Szklarz, G. D. & Scott, E. E. Human Cytochrome P450 1A1 structure and utility in understanding drug and xenobiotic metabolism. *J. Biol. Chem.* **288**, 12932–12943 (2013).
88. Wang, A., Savas, U., Stout, C. D. & Johnson, E. F. Structural characterization of the complex between α-Naphthoflavone and human Cytochrome P450 1B1. *J. Biol. Chem.* **286**, 5736–5743 (2011).
89. Marciniec, K. et al. Synthesis, anti-breast cancer activity, and molecular docking study of a New Group of Acetylenic Quinolinesulfonamide Derivatives. *Molecules* **22**, 300 (2017).

90. Morris, G. M. et al. AutoDock4 and AutoDockTools4: Automated docking with selective receptor flexibility. *J. Comput. Chem.* **30**, 2785–2791 (2009).
91. Trott, O. & Olson, A. J. AutoDock Vina: Improving the speed and accuracy of docking with a new scoring function, efficient optimization, and multithreading. *J. Comput. Chem.* **31**, 455–461 (2010).
92. Krieger, E. et al. Improving physical realism, stereochemistry, and side-chain accuracy in homology modeling: Four approaches that performed well in CASP8. *Proteins Struct. Funct. Bioinforma.* **77**, 114–122 (2009).
93. Sousa Da Silva, A. W. & Vranken, W. F. ACPYPE - AnteChamber PYthon Parser interfacE. *BMC Res. Notes* **5**, 367 (2012).
94. Wang, J., Wolf, R. M., Caldwell, J. W., Kollman, P. A. & Case, D. A. Development and testing of a general amber force field. *J. Comput. Chem.* **25**, 1157–1174 (2004).
95. Cabrera, N. et al. Searching glycolate oxidase inhibitors based on QSAR, molecular docking, and molecular dynamic simulation approaches. *Sci. Rep.* **12**, 19969 (2022).
96. Van Der Spoel, D. et al. GROMACS: Fast. *Flex. Free. J. Comput. Chem.* **26**, 1701–1718 (2005).
97. Kumari, R. & Kumar, R. Open Source Drug Discovery Consortium & Lynn, A. *g_mmpbsa* —A GROMACS tool for high-throughput MM-PBSA calculations. *J. Chem. Inf. Model.* **54**, 1951–1962 (2014).

Acknowledgements

The authors thank the Pontificia Universidad Católica del Ecuador for funding through the project “Chemical profile and antioxidant capacity of Pourouma cecropiifolia Mart. from the Ecuadorian Amazon” [grant number: 007-UIO-2023]. The authors also would like to thank the Central University of Ecuador for funding the purchase of reagents necessary for the development of this project.

Author contributions

Conceived the project, P.J.E.-M.; visualization, P.J.E.-M., C.M.-D., P.A.C.-P., J.C.R.-B., and L.F.; investigation, P.J.E.-M., C.M.-D., P.A.C.-P., J.C.R.-B. and L.F.; performed the experiments, C.M.-D., R.M.-S., N.G.S.M., S.A.C., J.C.R.-B., D.R.-F. and N.B.-M.; supervision, P.J.E.-M.; data analysis, N.B.-M., N.G.S.M., P.A.C.-P., J.C.R.-B., R.M.-S., C.M.-D., D.R.-F. and L.F.; conducted and analyzed the molecular docking part, S.A.C. and J.R.M.; writing—original draft preparation, P.J.E.-M., C.M.-D., N.G.S.M., J.R.M., and P.A.C.-P.; writing—review and editing, P.J.E.-M., C.M.-D., N.G.S.M., J.R.M., N.B.-M., S.A.C., L.F., and P.A.C.-P.; project administration, P.J.E.-M., funding acquisition; P.J.E.-M.

Competing interests

The authors declare no competing interests.

Additional information

Supplementary information The online version contains supplementary material available at https://doi.org/10.1038/s41538-025-00503-x.

Correspondence and requests for materials should be addressed to Patricio J. Espinoza-Montero.